Analysis of ultrafiltration models: influence of operational conditions.

María-Cinta Vincent-Vela, Beatriz Cuartas-Uribe, Silvia Álvarez-Blanco*, Jaime Lora-García

Department of Chemical and Nuclear Engineering, Universidad Politécnica de Valencia, C/Camino de Vera s/n 46022 Valencia, Spain.

Abstract:

Ultrafiltration is a widely used technique to remove hazardous pollutants from wastewaters. Membrane dynamic ultrafiltration (UF) models have been widely investigated and described in the literature. The main equations of most of the dynamic ultrafiltration models found in the literature can be linearized to obtain an equation expressed in terms of TMP^2/J_P^2, as a function of time. In this work, experimental results from ultrafiltration tests are expressed in terms of TMP^2/J_P^2 as a function of time. TMP, feed concentration (FC), temperature and crossflow velocity (CFV) were studied. The feed consisted in an aqueous solution of polyethylene glycol (PEG) of 35 Kg/mol. The results showed a linear variation in TMP^2/J_P^2 with time. For severe fouling conditions, the linearity found in the initial membrane fouling resistance with TMP was also the highest. A linear correlation between the initial membrane fouling resistance and the temperature was also found for the experimental conditions tested. However, it was found that, above a certain temperature, increasing temperature did not result in a noticeable reduction of the gel layer resistance. Linear models for steady state permeate flux and r_c/c_g as a function of TMP and CFV were also obtained.

*Corresponding author, *Tel. +34 963877000x76383 fax: +34 963877639*
E-mail: sialvare@iqn.upv.es (S. Álvarez-Blanco)

Keywords: Model; Ultrafiltration; Initial membrane fouling resistance; Gel layer.

1. Introduction

Membrane technologies are widely used in a lot of chemical processing industries as well as in wastewater treatment. For this reason, the study of the main problems in these processes is very important to optimise the operating conditions and to reduce environmental problems. One of the critical factors governing membrane technologies in industrial processing is membrane fouling. Membrane fouling is responsible for permeate flux decline and it contributes to a reduction in the productivity in chemical processing industries. It also implies a diminution of the efficiency of wastewater treatments. [1-2].

Ultrafiltration uses a finely porous membrane to separate water and microsolutes from macromolecules and colloids [3]. These waste streams contain compounds that are highly hazardous materials when they are released to the environment. There are many examples of highly hazardous pollutants removal with ultrafiltration processes in the literature. Tansel et al. [4] and Rezvanpour et al. [5] achieved pretroleum based chemicals removal from contaminated water streams by means of ultrafiltration. Rojas et al. [6] successfully applied ultrafiltration in the removal of viruses and bacteria from surface water destined for human consumption. Other authors studied the removal of heavy metals from aqueous wastestreams with micellar enhanced untrafiltration [7] and polymer assisted ultrafiltration processes [8, 9].

Fouling diminishes the efficiency of ultrafiltration. Therefore, mathematical modelling of fouling is very interesting. Polyethylene glycol was chosen as a model macromolecule to perform fouling experiments because it has been often used as a

standard macromolecule to test fouling models. Macromolecular compounds are responsible for fouling problems in membrane processes, especially when ultrafiltration membranes are used

Mathematical modelling of membrane fouling reduces the number of experiments that are necessary to select the best operating conditions for minimizing membrane fouling in industrial and environmental applications. Consequently, it saves time and money. Besides, it also has environmental implications due to a significant save in membrane replacement. [10-15]

In order to evaluate membrane performance, it is important to identify the fouling mechanisms. In this way, a great number of mathematical models have been studied in the literature to describe the mechanism of transport and fouling through ultrafiltration membranes with macromolecular compounds. Membrane fouling can be analyzed using different models. Current UF models are based on three basic models: (i) the gel polarization model [16-18], (ii) the osmotic pressure model [19, 20], and (iii) the resistance-in-series model [21-23]. The gel polarization model considers that permeate flux decline is caused by the hydraulic resistance of the gel layer. In the osmotic pressure model, when there is an increase in the osmotic pressure of the retentate, the permeate flux is reduced. In the resistance-in-series model, three main resistances are responsible for permeate flux decline: the fouling resistance, the solute adsorption resistance and the concentration polarization resistance.

In this work, macromolecular solutions were ultrafiltered in a tubular membrane module to study permeate flux decline and fouling problems. This allowed to obtain a linear

equation in terms of transmembrane pressure (TMP) divided by permeate flux as a function of time. In addition, the quotient specific resistance of the gel layer divided by the gel layer concentration was also estimated. The effects of feed concentration (FC), crossflow velocity (CFV) and TMP on TMP^2/J_P^2 and r_c/C_g were reported.

2. Theory

Membrane dynamic ultrafiltration models have been widely investigated and described in the literature. Model predictions have been compared with experimentally obtained ultrafiltration results. The main equations of dynamic ultrafiltration models [1, 2, 24-28] can be linearized to obtain an equation expressed in terms of transmembrane pressure (TMP) divided by permeate flux, TMP^2/J_P^2, as a function of time (Eqs. (1-4)).

The main equation of the shear induced diffusion model [24, 28] is Eq. (1).

$$J_P = \frac{\dfrac{TMP}{\mu \cdot R_m}}{\left(1 + 2 \cdot \beta \cdot \dfrac{t - \dfrac{D \cdot \left(C_{gv} - C_{0v} - C_{0v} \cdot \ln\left(\dfrac{C_g}{C_0}\right)\right)}{\dfrac{TMP^2}{\left(\mu \cdot R_m\right)^2}}}{\dfrac{C_g - C_0}{C_0} \cdot \dfrac{\dfrac{D_h}{2}}{\dfrac{TMP}{\mu \cdot R_m}}}\right)^{-1/2}} \tag{1}$$

where J_P is the permeate flux (m s^{-1}), TMP is the transmembrane pressure (Pa), μ is the dynamic viscosity of the permeate (kg $m^{-1}s^{-1}$), R_m is the membrane resistance (m^{-1}), β is

the dimensionless resistance of the cake layer, D is the solute diffusivity (m^2s), C_{0v} is the solute concentration in the feed expressed in volume per volume, C_{gv} is the solute concentration in the gel layer in volume per volume, C_0 is the feed concentration (kg m^{-3}), C_g is the gel layer concentration (kg m^{-3}), D_h is the hydraulic diameter of the membrane (m) and t is time (s).

Another model whose main equation (Eq. (2)) can be linearized is a model that was developed for dead-end ultrafiltration and afterwards adapted to crossflow UF [25, 28]. According to the model, flux decline with time is described by Eq. (2).

$$J_P = \frac{TMP}{\mu \cdot R_m} \cdot \left(1 + 2 \cdot R'_c \cdot \frac{TMP}{\mu \cdot R_m{}^2} \cdot \frac{C_0}{C_g - C_0} \cdot t \right)^{-\frac{1}{2}} \quad (2)$$

In Eq. (2) R'_c is the specific resistance of the cake layer (m^{-2}).

The model that considers that ultrafiltration is a dynamic process that changes from a non equilibrium condition to an equilibrium condition, in which the cake layer thickness remains constant [2], can also be linearized in terms of TMP^2/J_P^2 as a function of time. This is one of the most accepted models that describe crossflow ultrafiltration. The main equation of this model corresponds to Eq. (3).

$$J(t) = \frac{\left(TMP - \Delta P_c\right)}{\mu R_0} \left[1 + \frac{2 r_c \left(TMP - \Delta P_c\right)}{\mu^2 R_0^2} \frac{C_o}{C_g} t \right]^{-1/2} \quad (3)$$

In Eq. (3) R_0 is the initial membrane fouling resistance (m^{-1}), r_c is the specific resistance of the gel layer (kg $m^{-3}s^{-1}$) and ΔP_c is the critical pressure above which membrane fouling occurs (Pa).

Finally, a model based in the resistance in series model that integrates in the same analytical expression the osmotic pressure as well as gel layer formation [1, 27] and whose main equation is Eq. (4), can also be linearized as previously described.

$$J_P = \left(\frac{\mu^2 \left(R_m + R_a + R_{osm} \right)^2}{TMP^2} + \frac{2 \cdot a \cdot \mu \cdot C_0}{TMP} \cdot t \right)^{-1/2} \quad (4)$$

In Eq. (4) R_a is the adsorption resistance (m^{-1}), R_{osm} is the osmotic resistance (m^{-1}) and a is the specific resistance of the gel layer (m kg^{-1}).

In this work, experimental results from pilot plant ultrafiltration tests are expressed as TMP^2/J_P^2 versus time to check their linearity. Moreover, the parameters R_m and r_c/C_g are determined from the linearized Eq. (3).

3. Experimental

2.1. Membranes

The membranes used in the ultrafiltration tests were monotubular TiO_2/Al_2O_3 ceramic membranes with a molecular weight cut-off (MWCO) of 5 kg/mol from Tami Industries (France). Membrane area was 35.25 cm^2.

2.2. Ultrafiltration tests

Transmembrane pressure (TMP), feed concentration, temperature and crossflow velocity were varied in the interval of 0.2 to 0.5 MPa, 5 to 15 g/L, 15 to 40ºC and 1 to 3 m/s for TMP, feed concentration, temperature and crossflow velocity, respectively. The feed consisted in an aqueous solution of polyethylene glycol (PEG) of 35 Kg/mol. Ultrafiltration tests were performed with the ultrafiltration pilot plant described elsewhere [24].

2.3. Membrane cleaning protocol

Membrane cleaning was performed at 40 ºC with a 0.25 g/L NaClO aqueous solution (pH 11 by NaOH addition). As the cleaning protocol was optimum, the same membrane was used in all the experiments.

4. Results and discussion

Figs. 1-2 show the experimental data obtained in the ultrafiltration experiments for the lowest crossflow velocity tested, 1 m/s. The experimental data is plotted in terms of TMP^2/J_P^2 as a function of time, according to the linearized expressions of some of the ultrafiltration models found in the literature [1, 2, 29]. The results show that even for low crossflow velocities, which are the experimental conditions for which membrane fouling is more severe, the variation in TMP^2/J_P^2 with time is linear. This is consistent with the equations of most ultrafiltration models.

For a feed concentration of 15 g/L (Fig. 2), linearity of TMP^2/J_P^2 with time is also observed. However, this tendency is not followed by experimental data in the earliest

stages of ultrafiltration for high TMPs. This behaviour was also observed in the ultrafiltration of PEG solutions with Carbosep membranes at a feed concentration of 5 g/L [29]. This may be attributed to the fact that some other fouling mechanisms not considered in the models, such as pore blocking, are occurring for short time scales. These mechanisms have more influence on membrane performance in the case of the Carbosep membranes used in this work than in the case of the Tami membranes used in this work. It can be observed that non-linearity at the beginning of ultrafiltration appears at lower feed concentrations in the case of Carbosep membranes.

Fig. 3 confirms that the linear tendency observed for TMP^2/J_P^2 with time is maintained when the temperature is varied from 15ºC to 40 ºC for a feed concentration of 5 g/L under the more severe fouling conditions tested: a crossflow velocity of 1 m/s and a TMP of 0.5 MPa.

The results of the regression analysis are used to estimate the initial membrane fouling resistance, R_0, and the relation r_c/C_g. These values are given in Figs. 4-9. Figs. 4-5 show that the linearity found in the initial membrane fouling resistance with TMP increases when the experimental conditions are more favourable to cause severe membrane fouling, i.e. for low crossflow velocities and high feed concentrations. In addition, the initial membrane fouling resistance increases with TMP for all the experimental conditions tested except in the case of high crossflow velocities and low TMPs and feed concentrations. These conditions correspond to the mildest fouling conditions.

Fig. 6 illustrates the variation of the initial membrane fouling resistance with temperature for a feed concentration of 5 g/L under the more severe fouling conditions

tested: a crossflow velocity of 1 m/s and a TMP of 0.5 MPa. The initial membrane fouling resistance decreases with an increase in temperature due to a decrease in the viscosity of the feed solution. Low viscosity values contribute to create milder fouling conditions for the membrane. A linear relationship of the initial membrane fouling resistance with temperature is found for the experimental conditions tested.

Figs. 7-8 show the quotient r_c/C_g versus TMP for all the crossflow velocities tested and feed concentrations of 5 and 15 g/L. Previous works with Carbosep membranes [30] showed that the quotient r_c/C_g always increased with TMP. However, in the case of Tami membranes (Figs. 7-8) the results showed that r_c/C_g first decreases with TMP and then it increases for high TMPs. These results can be explained considering the relations between r_c/C_g, membrane MWCO and PEG molecular weight. In the case of the Carbosep membrane, as TMP increases C_g decreases because some PEG molecules are capable of passing through the membrane (PEG retention 85% approximately) [24]. Moreover, for high TMP, gel layer compaction occurs, and as a result r_c increases. Concerning to Tami membrane at low TMP, as TMP increases C_g increases as well because the Tami membrane rejects nearly all PEG molecules (PEG retention higher than 99%). However, at high TMP, r_c increases with TMP because there is gel layer compaction. For low crossflow velocities and low TMPs (Figs. 7-8), the decrease in r_c/C_g with an increase in TMP is small compared to the one observed for high crossflow velocities. Moreover, for low crossflow velocities and high TMPs the increase in r_c/C_g with an increase in TMP is greater than the increase observed for high crossflow velocities, especially in the case of high feed concentrations.

Fig. 9 illustrates the variation of r_c/C_g with the temperature for a feed concentration of 5 g/L, a crossflow velocity of 1 m/s and a TMP of 0.5 MPa. It can be observed that an increase in the temperature results in a decrease in the gel layer resistance as a consequence of a decrease in the feed solution viscosity with temperature. However, the decrease in the feed solution viscosity with temperature does not result in a significant decrease of the gel layer resistance above 30 ºC. Therefore, a further increase in temperature does not contribute to substantially reduce membrane fouling for the experimental conditions tested.

Multiple linear regression models were fitted for the dependent variables TMP^2/J_{Pss}^2 and r_c/c_g (J_{Pss} refers to the steady-state permeate flux). The independent variables considered were TMP and CFv. In the multiple regression analysis, the models were modified by dropping the non-statistically significant terms. This was performed considering the p-values that correspond to each term of the model. The fitted models are shown in Table 1. The best fittings are obtained for the Carbosep membrane. For both membranes, the best fittings for TMP^2/J_{Pss}^2 as a function of TMP and CFv are obtained for low feed concentrations. This means that, at low feed concentrations, the relationship between TMP^2/J_{Pss}^2 and TMP and CFv is linear, whereas it becomes non-linear at higher feed concentrations. In the case of r_c/c_g, the fitting was not very good, presumably because lineal models do not completely explain the dependence of r_c/c_g with TMP and CFv.

5. Conclusions

The results showed that even for low crossflow velocities and high feed concentrations, which are the experimental conditions for which membrane fouling is more severe, the

variation in TMP^2/J_P^2 with time was linear. This is consistent with the linearized expressions of most of the ultrafiltration models found in the literature. Nevertheless, linearity was not observed in the early stages of the ultrafiltration experiments performed with high feed concentrations. This can be explained considering that some other fouling mechanisms not included in the models, such as pore blocking, were occurring for short time scales.

Severe fouling conditions, high TMPs and low crossflow velocities, resulted in a higher contribution of the gel layer resistance to membrane fouling. The linearity found in the initial membrane fouling resistance with TMP was also the highest in the case of severe fouling conditions, i.e. for low crossflow velocities and high feed concentrations.

A linear correlation between initial membrane fouling resistance and temperature was found for the experimental conditions tested. The initial membrane fouling resistance and the gel layer resistance decreased with an increase in temperature, as expected. However, it was found that, above a certain temperature, increasing temperature did not result in a noticeable reduction of the gel layer resistance.

Multiple regression analysis allowed to obtain steady state permeate flux and r_c/c_g as a function of TMP and CFV. The best fittings were obtained for J_{Pss} at low feed concentrations for both membranes.

6. Nomenclature

a — specific resistance of the gel layer (kg/ m^3)

C_0 — solute concentration in the feed solution (kg/ m^3)

C_{0v} — solute concentration in the feed (m^3/ m^3).

C_g — solute concentration in the gel layer (m^3/ m^3)

C_{gv} — gel layer concentration (kg/ m^3)

CFv — crossflow velocity (m/s)

D — solute diffusivity (m^2/s)

D_h — hydraulic membrane diameter (m)

J_P — permeate flux (m/s)

J_{Pss} — steady state permeate flux (m/s)

R_a — adsorption resistance (m^{-1})

R'_c — specific resistance of the cake layer (m^{-2})

r_c — specific resistance of the gel layer (kg/m^3·s)

R_m — membrane resistance (m^{-1})

R_o — initial membrane fouling resistance (m^{-1})

R_{osm} — osmotic resistance of the cake layer (m^{-2})

t — time (s)

TMP — transmembrane pressure (Pa)

ΔP_C — critical pressure (Pa)

Greek letters

μ — dynamic viscosity of the permeate (kg/m·s)

β — resistance of the cake layer (dimensionless)

References

[1] S. Bhattacharjee, P.K. Bhattacharya, Flux decline behaviour with low molecular weight solutes during ultrafiltration in an unstirred batch cell, J. Membr. Sci. 72 (1992) 149-161

[2] L. Song, Flux decline in crossflow microfiltration and ultrafiltration: mechanisms and modeling of membrane fouling, J. Membr. Sci. 139 (1998) 183-200.

[3] R.W. Baker, Membrane technology and applications, John Wiley and Sons, Chichester, England, 2004.

[4] B. Tansel, J. Regula, R. Shalewitz, Evaluation of Ultrafiltration Process Performance for Treatment of Petroleum Contaminated Waters, Water Air Soil Pollut. 126 (2001) 291-305.

[5] A. Rezvanpour, R. Roostaazad, M. Hesampour, M. Nyström, C. Ghotbi, Effective factors in the treatment of kerosene–water emulsion by using UF membranes, J. Hazard. Mater. 161 (2009) 1216–1224.

[6] J.C. Rojas, B. Moreno, G. Garralón, F. Plaza, J. Pérez, M.A. Gómez, Potabilization of low NOM reservoir water by ultrafiltration spiral wound membranes, J. Hazard. Mater. 158 (2008) 593–598.

[7] V.D. Karate, K.V. Marathe, Simultaneous removal of nickel and cobalt from aqueous stream by cross flow micellar enhanced ultrafiltration, J. Hazard. Mater. 157 (2008) 464–471.

[8] J. Zeng, H. Ye, Z. Hu, Application of the hybrid complexation–ultrafiltration process for metal ion removal from aqueous solutions, J. Hazard. Mater. 161 (2009) 1491–1498.

[9] C. Cojocaru, G. Zakrzewska-Trznadel, A. Miskiewicz, Removal of cobalt ions from aqueous solutions by polymer assisted ultrafiltration using experimental design approach Part 2: Optimization of hydrodynamic conditions for a crossflow ultrafiltration module with rotating part, J. Hazard. Mater. 169 (2009) 610–620.

[10] H.M. Yeh, J.H. Dong, M.Y. Shi, Momentum balance analysis of flux and pressure declines in membrane ultrafiltration along tubular modules, J. Membr. Sci. 241 (2004) 335-345.

[11] T. Furukawa, K. Kokubo, K. Nakamura, K. Matsumoto, Modeling of the permeate flux decline during MF and UF cross-flow filtration of soy sauce lees, J. Membr. Sci. 322 (2008) 491-502.

[12] S. Nataraj, R. Schomäcker, M. Kraume, I.M. Mishra, A. Drews, Analyses of polysaccharide fouling mechanisms during crossflow membrane filtration, J. Membr. Sci. 308 (2008) 152-161.

[13] S.T.D. de Barros, C.M.G. Andrade, E.S. Mendes, L. Peres, Study of fouling mechanism in pineapple juice clarification by ultrafiltration, J. Membr. Sci. 215 (2003) 213-224.

[14] M.K. Purkait, P.K. Bhattacharya, S. De, Membrane filtration of leather plant effluent: Flux decline mechanism, J. Membr. Sci. 258(2005)85-96.

[15] H. Peng, A.Y. Tremblay, Membrane regeneration and filtration modeling in treating oily wastewaters, J. Membr. Sci. 324 (2008) 59-66.

[16] H.M. Yeh, T.W. Cheng, J.W. Tsai, Modified concentration polarization model for hollow-fiber membrane ultrafiltration, Sep. Purif. Technol. 16 (1999) 189-192.

[17] Mohd.Z. Sulaiman, N.M. Sulaiman, B. Abdellah, Prediction of dynamic permeate flux during cross-flow ultrafiltration of polyethylene glycol using concentration polarization-gel layer model, J. Membr. Sci. 189 (2001) 151-165.

[18] S.K. Karode, A method for prediction of the gel concentration in macromolecular ultrafiltration. J. Membr. Sci. 171 (2000) 131-139.

[19] Ko M.K., Pellegrinox J.J, Determination of osmotic pressure and fouling resistance and their effects of performance of ultrafiltration membranes, J. Membr. Sci. 74 (1992) 141-157.

[20] H.M. Yeh, T.W. Cheng, Osmotic-pressure model with permeability analysis for ultrafiltration in hollow-fiber membrane modules, Sep. Technol. 3 (1993) 91-98.

[21] P. Rai, C. Rai, G.C. Majumdar, S. DasGupta, S. Dex, Resistance in series model for ultrafiltration of mosambi (Citrus sinensis (L.) Osbeck) juice in a stirred continuous mode, J. Membr. Sci. 283 (2006) 116-122.

[22] R.S. Juang, H.L. Chen, Y.S. Chenx, Resistance-in-series analysis in cross-flow ultrafiltration of fermentation broths of Bacillus subtilis culture, J. Membr. Sci. 323 (2008) 193-200.

[23] T.W. Cheng, H.M. Yeh, C.T. Gau, Flux analysis by modified osmotic-pressure model for laminar ultrafiltration of macromolecular solutions, Sep. Purif. Technol. 13 (1998) 1-8.

[24] M.C. Vincent-Vela, S. Álvarez-Blanco, J. Lora-García, J.M. Gozálvez-Zafrilla, E. Bergantiños-Rodríguez, Utilization of a shear induced diffusion model to predict permeate flux in the crossflow ultrafiltration of macromolecules, Desalination 206 (2007) 61-68.

[25] M.C. Vincent-Vela, S. Álvarez-Blanco, J. Lora-García, Crossflow ultrafiltration of cake forming solutes: a non-steady state model, Desalination. 184 (2005) 347-356.

[26] M.C. Vincent-Vela, S. Álvarez-Blanco, J. Lora-García, E. Bergantiños-Rodríguez, Prediction of flux decline in the ultrafiltration of macromolecules, Desalination 192 (2006) 323-329.

[27] M.C. Vincent-Vela, S. Álvarez-Blanco, J. Lora-García, J.M. Gozálvez-Zafrilla, E. Bergantiños-Rodríguez, Modelling of flux decline in crossflow ultrafiltration of macromolecules: comparison between predicted and experimental results, Desalination 204 (2007) 328-334.

[28] R.H. Davis, Modeling of fouling of crossflow microfiltration membranes, Sep. Purif. Methods 21(1992) 75-126.

[29] M.C. Vincent-Vela, S. Álvarez-Blanco, J. Lora-García, J.M. Gozálvez-Zafrilla, E. Bergantiños-Rodríguez, Linerization of ultrafiltration models: analysis of experimental data from ultrafiltration tests, Desalination and Water treatment 10 (2009) 144-147.

[30] M.C. Vincent-Vela, S. Álvarez-Blanco, J. Lora-García, E. Bergantiños-Rodríguez, Analysis of membrane pore blocking models adapted to crossflow ultrafiltration in the ultrafiltration of PEG, Chem. Eng. J. 149 (2009) 232–241.

Table 1. Multiple linear regression models for TMP^2/J_{Pss}^2 and r_c/c_g.

Membrane	FC (g/L)	Equations of the models	R^2	p-Value of the model
TAMI	5	$TMP^2/J_{Pss}^2 = 1.445\cdot10^{21} - 7.434\cdot10^{21}\cdot TMP + 1.145\cdot10^{22}\cdot TMP^2 + 6.020\cdot10^{20}\cdot CFV - 1.505\cdot10^{20}\cdot CFV^2$	92.67	0.0005
	5	$r_c/c_g = 1.109\cdot10^{10} + 6.647\cdot10^{10}\cdot TMP^2 - 4.823\cdot10^{10}\cdot TMP - 1.170\cdot10^{9}\cdot TMP\cdot CFV$	69.85	0.0177
	15	$TMP^2/J_{Pss}^2 = 1.596\cdot10^{22} - 1.248\cdot10^{22}\cdot CFV + 2.073\cdot10^{21}\cdot CFV^2 + 3.986\cdot10^{21}\cdot TMP\cdot CFV$	63.18	0.0380
	15	$r_c/c_g = 7.792\cdot10^{9} + 3.129\cdot10^{10}\cdot TMP^2 - 9.922\cdot10^{9}\cdot TMP\cdot CFV$	79.09	0.0009
Carbosep	5	$TMP^2/J_{Pss}^2 = 1.300\cdot10^{20} + 3.897\cdot10^{21}\cdot TMP - 4.046\cdot10^{20}\cdot CFV - 1.209\cdot10^{21}\cdot TMP\cdot CFV + 1.250\cdot10^{20}\cdot CFV^2$	97.63	0.0000
	5	$r_c/c_g = -3.508\cdot10^{9} + 4.291\cdot10^{10}\cdot TMP + 5.107\cdot10^{8}\cdot CFV^2 - 1.551\cdot10^{10}\cdot TMP\cdot CFV$	90.44	0.0002

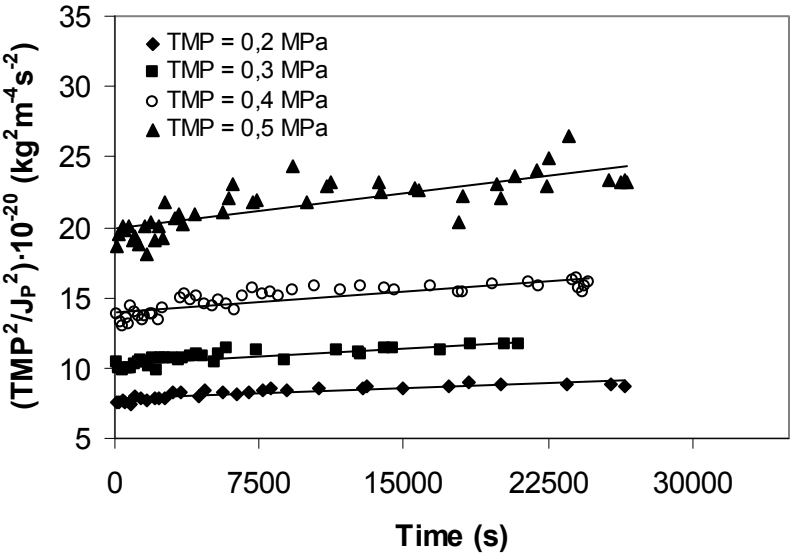
TMP = 0,2 MPa
TMP = 0,3 MPa
TMP = 0,4 MPa
TMP = 0,5 MPa
(TMP²/Jp²)·10⁻²⁰ (kg²m⁻⁴s⁻²)
Time (s)
35
30
25
20
15
10
5
0
7500
15000
22500
30000

Fig. 1.

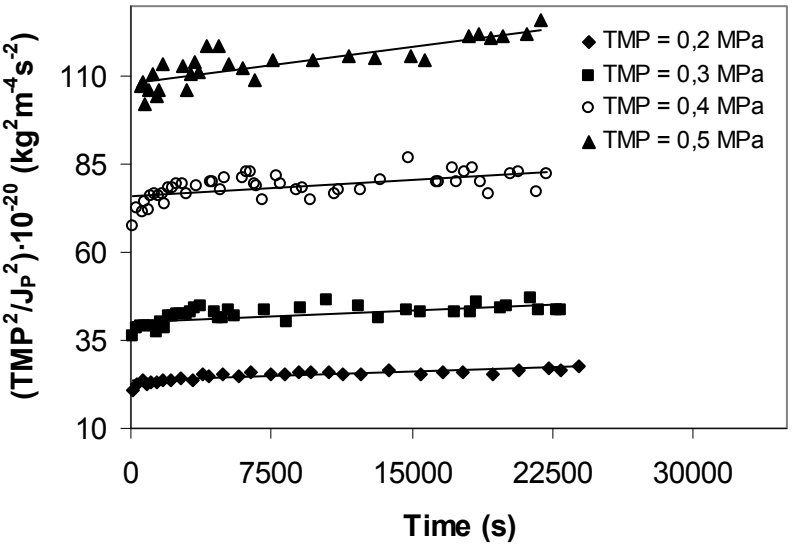
TMP = 0,2 MPa
TMP = 0,3 MPa
TMP = 0,4 MPa
TMP = 0,5 MPa
(TMP²/Jp²)·10⁻²⁰ (kg²m⁻⁴s⁻²)
Time (s)
110
85
60
35
10
0
7500
15000
22500
30000

Fig. 2.

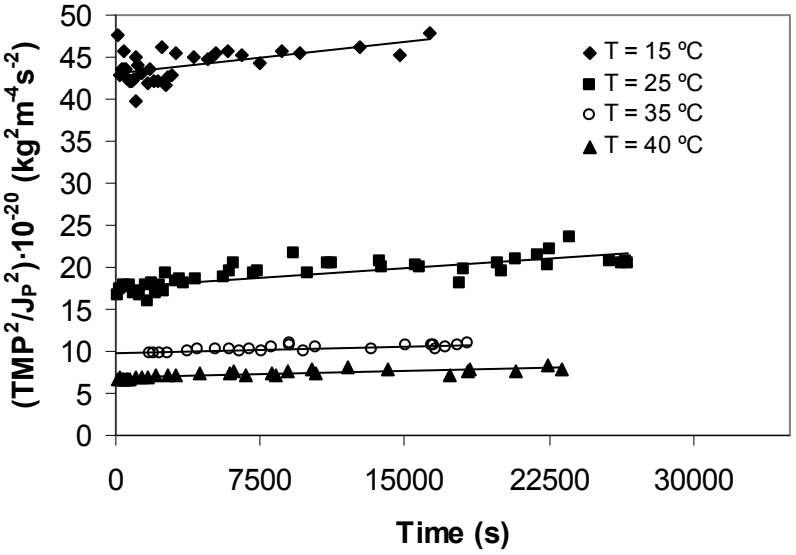
50
45
40
35
30
25
20
15
10
5
0
0
7500
15000
22500
30000
Time (s)
(TMP²/Jp²)·10⁻²⁰ (kg²m⁻⁴s⁻²)
T = 15 ºC
T = 25 ºC
T = 35 ºC
T = 40 ºC

Fig. 3.

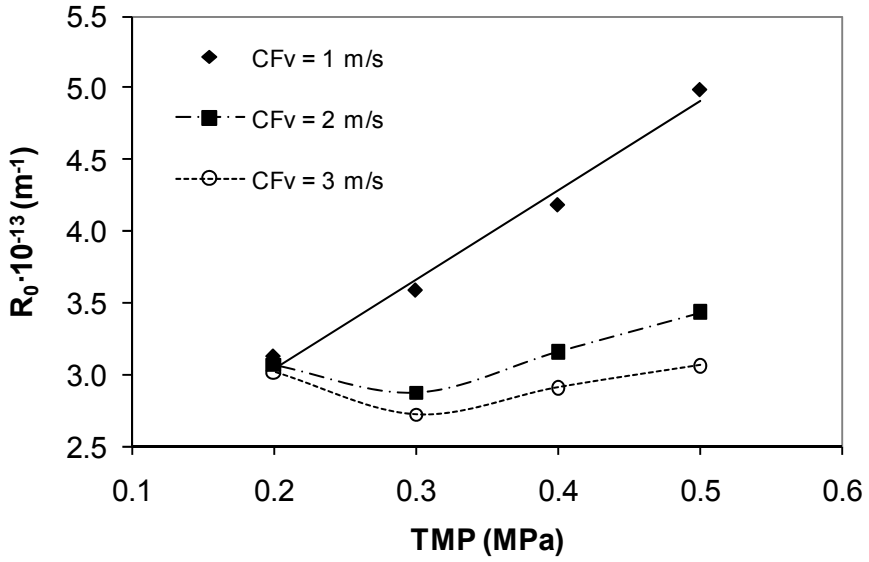
5.5
5.0
4.5
4.0
3.5
3.0
2.5
0.1
0.2
0.3
0.4
0.5
0.6
TMP (MPa)
R₀·10⁻¹³ (m⁻¹)
CFv = 1 m/s
CFv = 2 m/s
CFv = 3 m/s

Fig. 4.

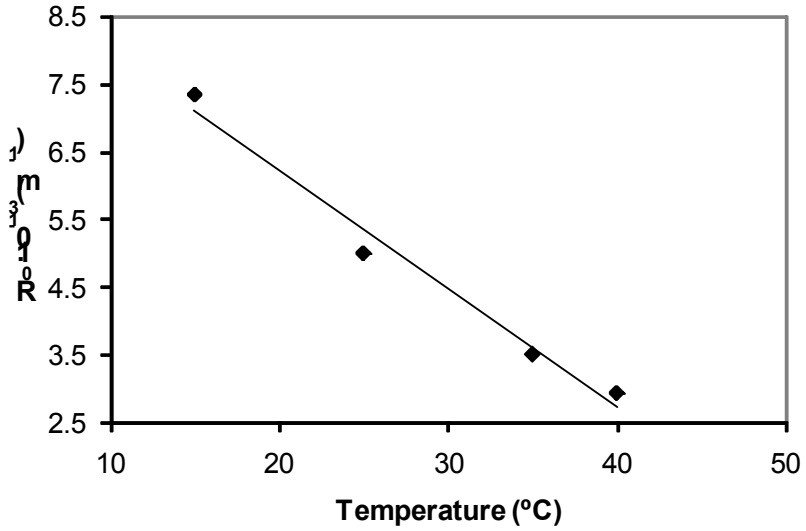
8.5
7.5
6.5
5.5
4.5
3.5
2.5
10
20
30
40
50
Temperature (ºC)

Fig. 6.

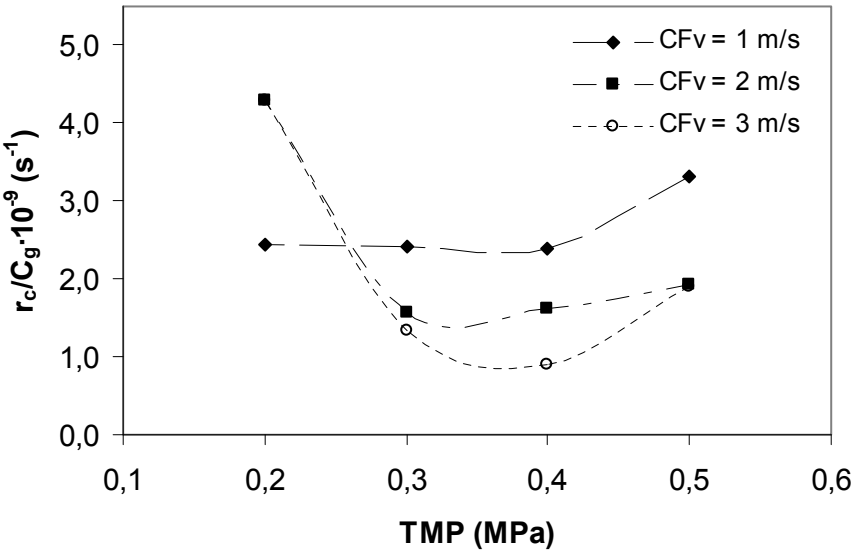
CFv = 1 m/s
CFv = 2 m/s
CFv = 3 m/s
5,0
4,0
3,0
2,0
1,0
0,0
0,1
0,2
0,3
0,4
0,5
0,6
TMP (MPa)

Fig. 7.

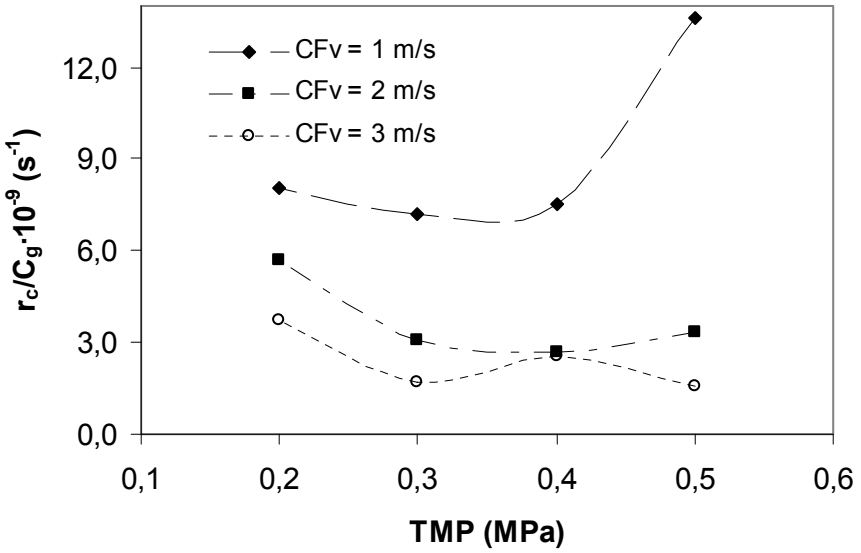

Fig. 8.

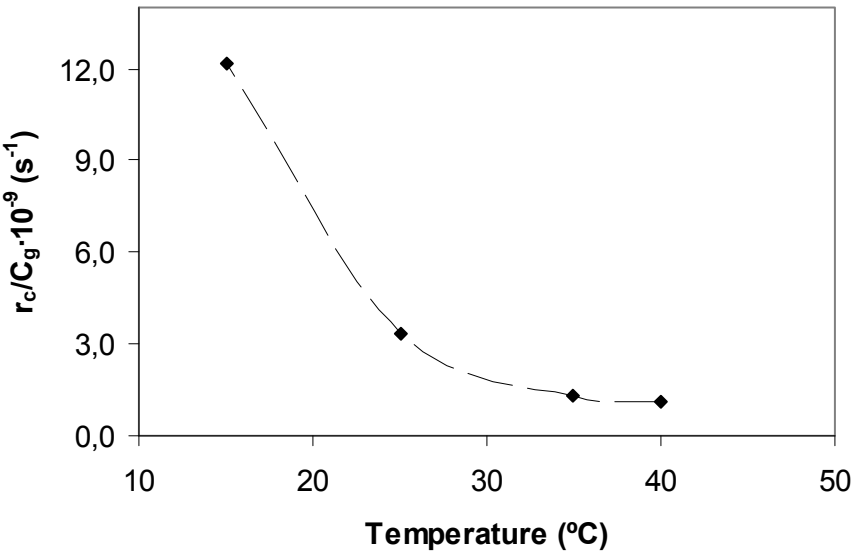

Fig. 9.

Fig. 1. Linear regression of experimental data according to linearized ultrafiltration models for a crossflow velocity of 1 m/s, a feed concentration of 5 g/L and a temperature of 25ºC.

Fig. 2. Linear regression of experimental data according to linearized ultrafiltration models for a crossflow velocity of 1 m/s, a feed concentration of 15 g/L and a temperature of 25ºC.

Fig. 3. Linear regression of experimental data according to linearized ultrafiltration models for a crossflow velocity of 1 m/s, a feed concentration of 5 g/L and a TMP of 0.5 MPa.

Fig. 4. Initial membrane fouling resistance for a feed concentration of 5 g/L and a temperature of 25ºC.

Fig. 5. Initial membrane fouling resistance for a feed concentration of 15 g/L and a temperature of 25ºC.

Fig. 6. Initial membrane fouling resistance for a feed concentration of 5 g/L, a crossflow velocity of 1 m/s and a TMP of 0.5 MPa.

Fig. 7. Relation r_c/C_g for a feed concentration of 5 g/L and a temperature of 25ºC.

Fig. 8. Relation r_c/C_g for a feed concentration of 15 g/L and a temperature of 25ºC.

Fig. 9. Relation r_c/C_g for a feed concentration of 5 g/L, a crossflow velocity of 1 m/s and a TMP of 0.5 MPa.